Int. J. Nano Dimens., 11 (3): 248-257, Summer 2020

ORIGINAL ARTICLE

Theoretical insights into the adsorption behavior of CO molecules on the pure and V_n-doped BN nanotubes

Batoul Makiabadi[1*], Mohammad Zakarianezhad[2], Abazar Azodi[2]

[1]Department of Chemical Engineering, Sirjan University of Technology, Sirjan, Iran
[2]Department of Chemistry, Payame Noor University, Tehran, Iran

Received 11 March 2020; revised 11 May 2020; accepted 20 May 2020; available online 26 May 2020

Abstract

Interaction of pure and Vn-doped (8, 0), (12, 0) and (16, 0) boron nitride nanotubes with CO molecules was studied using B3LYP/6-311++G(d) theoretical level. Substituting V instead of B atoms, increased the reactivity of nanotube. From the results, the complex stability depends on the direction and the number of the CO molecules interacted with the nanotube. In this work, the quantum molecular descriptors were used for the investigation of boron nitride nanotube reactivity to CO molecules both in the gas phase and in the solution. Also, the influence of the diameter of the nanotube on the electronic properties of the complexes was investigated. The charge transfer in complexes was calculated with NBO analysis. It is expected that Vn-doped nanotubes can be considered as a detector of CO gas molecules.

Keywords: *Boron Nitride Nanotube; Detector; Electronic Properties; HOMO-LUMO Gap; V-doped Nanotube.*

How to cite this article

Makiabadi B., Zakarianezhad M., Azodi A. Theoretical insights into the adsorption behavior of CO molecules on the pure and V_n-doped BN nanotubes. Int. J. Nano Dimens., 2020; 11 (3): 248-257.

INTRODUCTION

After the discovery of carbon nanotubes (CNTs) by Ijima [1], carbon nanotubes have attracted considerable attention in different fields due to their physical and chemical properties [2,3]. carbon nanotubes can be used as prime materials for gas adsorption, biological, chemical, and electromechanical sensors, and nanoelectronic devices [4-7]. CNTs can be metallic or semiconducting, and this behavior of CNTs depends on the diameter and chirality of nanotubes, which makes limiting the use of these nanotubes in various fields [8]. Therefore, many investigations have been performed to synthesize and modeling nanotubes independent of these factors [9]. Finally, boron nitride nanotubes (BNNTs) were synthesized after they were computationally stabilized [10]. In contrast to the CNTs, the boron nitride nanotubes have a semiconductor property that is independent of tubular diameter and helicity. Also, the boron nitride nanotubes are chemically and thermally more stable than the CNTs [11,12]. Unlike carbon nanotubes, BNNTs are noncytotoxic and are predicted that these nanotubes to be suitable in various medical fields relative to the CNTs [13,14]. The boron nitride nanotubes because of their physicochemical and electronic properties can be used as gas storage, catalysis, molecular sensing, field emission displayer, and drug delivery [15-21]. On the other hand, the high band gap and the low dissolution have limited the use of them. The investigations show that defect or doping, enhances the application of BNNTs in different fields such as nanoelectronics, nanoscale biotechnology, and biosensors [22-25]. The doping effect of the elements on the adsorption of the various molecules on the BNNTs was investigated by the theoretical methods [26-28].

Carbon monoxide (CO) is a colorless, odorless, and a tasteless flammable gas. CO is a conventional

* Corresponding Author Email: *bmakiabadi@yahoo.com*

toxic gas in the atmosphere that mostly produced by automobiles and industrial processes. Many investigations have been performed on the CO adsorption on the pure and doped carbon nanotubes [29-32]. For instance, Hamadanian *et al.* shown that Al-doped (10, 0) carbon nanotubes presents an excellent sensitivity to CO, compared with the pure carbon nanotubes [29]. Also, many studies on the interaction of the CO molecule with pure and doped born nitride nanotubes were done and indicate that pure BNNTs are not reactive to CO, but after doping, the reactivity remarkably increased [33-37]. In this work, we selected the V-doped BNNTs and investigated the interaction of Co molecules with the V-doped BN nanotubes. Analysis of the electronic properties of the structures was also investigated in the solution phase. Various researches show that the solvents can cause extensive changes in the molecular behaviors through the interactions between solute and solvent [38-40]. The main aim of this work is the study of the influence of the CO molecule interaction on the different properties of V_n-doped BNNTs. In this project, the effect of the number of doped vanadium atoms and the effect of the number of the CO molecules in addition to increasing the diameter of the nanotube has been investigated. The results of this study are useful for designing and developing of CO detectors.

COMPUTATIONAL METHODS

All structures were optimized at the level of density functional theory (DFT) with B3LYP exchange functional [41] and 6-311++G(d) basis set [42] using the Gaussian 09 software package [43]. The interaction energy (ΔE) was calculated as follows:

$$\Delta E = ET[CO/BNNT + nCO] - ET[BNNT] - nET[CO] \quad (1)$$

where ET[CO/BNNT + nCO] is the total energy of nanotube, n is the number of CO molecules, ET[BNNT] is the total energy of isolated tube and ET[CO] is the total energy of a CO molecule. The basis set superposition error (BSSE) was considered by counterpoise procedure for the correction of the interaction energies [44]. For all structures, the molecular descriptors such as the energy gap (Eg), the electronic chemical potential (μ), chemical hardness (η), chemical softness (S), electrophilicity index (ω) and the maximum amount of electronic charge of the system (ΔN_{max}) were evaluated at the B3LYP/6-311++G(d) level of theory. The energy gap (Eg), μ and η are defined as the following equation.

$$Eg=(E_{LOMU}-_{HOMO}),\ \mu=(E_{HOMO}+E_{LUMO})/2,\ \eta= -(E_{HOMO}-E_{LUMO})/2)) \quad (2)$$

where HOMO is the highest occupied molecular orbital and LUMO is the lowest unoccupied molecular orbital, respectively. Parameters S and ω are defined as the following equations, respectively.

$$S= (1/2\ \eta) \quad (3)$$

$$\omega= (\mu^2/2\eta) \quad (4)$$

The maximum amount of electronic charge (ΔN_{max}) that the electrophone system may accept was calculated as equation (5) [45].

$$\Delta N_{max} =(-\mu/\eta) \quad (5)$$

The polarizable continuum model (PCM) was examined for the investigation of the solvent effect on the physicochemical properties of complexes [46]. This model is a continuum solvent model well-developed and widely used in treating solvent effects on molecular properties. The charge analysis was performed at the B3LYP/6-311++G(d) level of theory using the NBO analysis [47]. Also, GaussSum program was used for the calculation of electron density of states (DOS) [48].

RESULTS AND DISCUSSION

Interaction of The CO molecules with pure and V_n-doped BNNTs

In this study, (8, 0), (12, 0) and (16, 0) boron nitride nanotubes were chosen (Fig. 1).

We have examined all the possible positions for CO molecules adsorption on the boron nitride nanotubes. The interaction of the CO molecule with BNNTs includes two kinds of configurations (**a** and **b**). In configurations **a** and **b**, C or O atom of CO interacted with B atom of the nanotube, respectively. Optimized structures of pure nanotubes and (8, 0) BNNT complexes are shown in Fig. 2.

In **a** and **b** configurations, the equilibrium distances of C…B and O…B were observed between CO and nanotubes, respectively. The equilibrium distances between CO and nanotubes and the interaction energies of the complexes are given in Table 1. The results indicate that the equilibrium distances of the **a** configurations are smaller than **b** configuration. Also, these equilibrium distances increased with increasing the tube diameter.

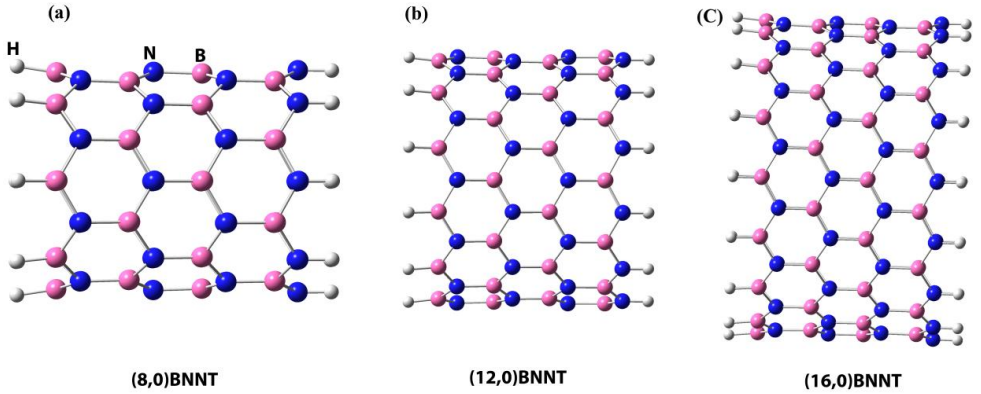

Fig. 1. Optimized structures of (a) (8,0)BNNT, (b) (12,0)BNNT, and (c) (16,0)BNNT.

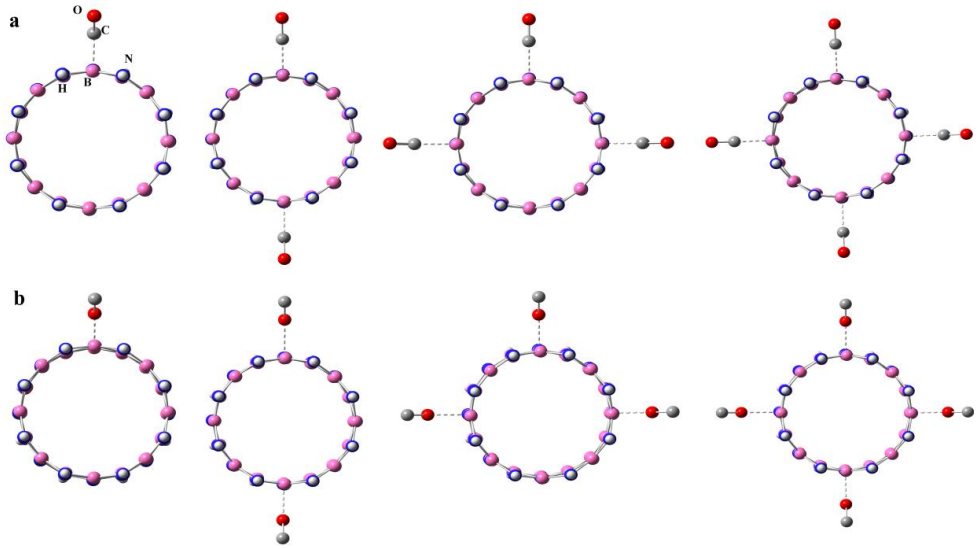

Fig. 2. Optimized structures for a and b configurations of $(CO)_n$/(8,0) BNNT complexes, (n=1-4).

Table 1. The interaction energy (kJ/mol), the O(C)…B distances (d), and the value of charge transfer (CT) from CO to nanotube for $(CO)_n$/BNNT complexes at the B3LYP/6-311++G(d) level of theory.

Complex	ΔE^{BSSE}	d/(Å)	CT		ΔE^{BSSE}	d/(Å)	CT		ΔE^{BSSE}	d/(Å)	CT
BNNT		(8,0)				(12,0)				(16,0)	
$(CO)_1$/BNNT											
a	-7.927	3.142	0.020	a	-6.796	3.167	0.014	a	-6.084	3.210	0.013
b	-4.530	3.339	0.005	b	-3.178	3.219	0.006	b	-2.695	3.252	0.005
$(CO)_2$/BNNT											
a	-15.561	3.142	0.041	a	-13.449	3.176	0.028	a	-12.371	3.254	0.026
b	-7.565	3.162	0.014	b	-6.197	3.226	0.012	b	-9.578	3.270	0.014
$(CO)_3$/BNNT											
a	-23.512	3.081	0.059	a	-20.157	3.225	0.042	a	-18.686	3.211	0.039
b	-11.535	3.144	0.024	b	-16.222	3.234	0.027	b	-8.502	3.253	0.015
$(CO)_4$/BNNT											
a	-30.997	3.036	0.077	a	-26.174	3.192	0.056	a	-25.111	3.218	0.052
b	-14.383	3.146	0.034	b	-12.115	3.230	0.024	b	-12.155	3.248	0.020

Therefore, it is predicted that these interactions in the **a** configurations are stronger than the **b** configurations and become weaker by increasing the tube diameter. The interaction energies (ΔE) of different complexes were calculated as a difference between the energy of the complex and the sum of the monomers' energies (Table 1). The BSSE correction was calculated and was added to the interaction energies.

According to the results, the configuration **a** is more stable than the **b**. This stability decreased with increasing the tube diameter. Therefore, it is predicted that the nanotubes with smaller diameter are more appropriate for the adsorption of the CO molecules. Two, three and four absorbed CO on BNNTs were also investigated. The results show that the interaction energy was increased by increasing the number of CO molecules and was decreased with increasing the diameter of the tube, but the order of complexes stability was not changed. The equilibrium distances between CO molecules and nanotubes increased by increasing the diameter of the tube. Therefore, the interaction of CO molecules with BNNT became weaker by increasing the diameter of the tube and indicate that the adsorption is physical. These results are consistent with previous studies [49]. The electronic property of $(CO)_n/V_n$−BNNT complexes was also investigated, where n=1-4. The optimized structures of the most stable configuration of $(CO)_n/V_n$−BNNT complexes are depicted in Fig. 3.

After V_n-doping, significant changes were observed. The CO molecules were getting closer to the nanotube. In other words, in V_n-doped complexes, the equilibrium distances between CO molecules and nanotubes were significantly decreased. It indicates that in comparison to pure BNNTs, the CO molecules have a stronger interaction with V_n-doped BNNTs. Therefore, the CO molecules can be chemically adsorbed on the V_n-doped nanotubes. The interaction energies and the equilibrium distances of $(CO)_n/V_n$−BNNT complexes are given in Table 2.

Similar to BNNTs, the adsorption of CO molecules from the C head on the surfaces of V_n-BNNTs is more stable than the O head. The results show that the interaction energies corresponding to $(CO)_n/V_n$−BNNT complexes are more than $(CO)_n$/BNNT complexes. Therefore, the $(CO)_n/V_n$−BNNT complexes are more stable than $(CO)_n$/BNNT. It seems that V_n-BNNTs to be energetically more appropriate for the adsorption of CO molecules. In $(CO)_n/V_n$−BNNT complexes, the equilibrium distances of C…O and O…C decreased by increasing the number of CO or V and the diameter of the tube, while the interaction energies increased. Therefore, it is predicted that the large-diameter nanotubes to be more appropriate for the adsorption of CO gas molecules.

The effect of the number of CO absorbed on the electronic properties of BNNTs and V_n– BNNTs

To understand the effect of CO molecules adsorbed on the electronic properties of BNNTs and V_n- BN nanotubes, some of the quantum molecular descriptors for $(CO)_n$/BNNT and $(CO)_n/V_n$-BNNT complexes in the gas phase were investigated, and data were given in Tables 3 and 4, respectively.

The results show that in the interaction of CO molecules with BNNTs, the energy gap (Eg) of nanotubes decreased, and conductivity of the nanotubes increased upon complexation. Also, the chemical softness, chemical potential, electrophilicity index, and ΔN_{max} of the CO/BNNT complexes increased, and the chemical hardness decreased upon complexation. As can be seen, the value of the energy gap for **b** configurations is higher than **a** ones. Therefore, the stability and conductivity of **a** configurations are more than **b** ones. After the V-doping, the energy gap of BNNTs was reduced, and the conductivity of BNNTs was significantly increased (Table 4).

The results show that the energy gap and chemical hardness of $(CO)_n$/BNNTs are higher than those of $(CO)_n/V_n$−BNNT complexes. Also, chemical potential, chemical softness, ΔN_{max}, and electrophilicity index for $(CO)_n$/BNNTs are smaller than those of $(CO)_n/V_n$−BNNT complexes. Therefore, it is predicted that after the doping of BNNTs, the stability and conductivity of the complexes were increased. The electronic properties of BNNTs and $(CO)_n$/BNNTs complexes didn't significantly change by increasing the diameter of the tube and the number of CO molecules. But, in V_n-BNNTs, with increasing the diameter of the tube, the band gap energy and the chemical hardness of BNNTs decreased, and also their softness and reactivity increased. In V_n-BNNTs, with the same diameter, the energy gap and the chemical hardness of complexes decreased by increasing the number of CO molecules and V doped atoms. Therefore, chemical softness, chemical potential, electrophilicity index and ΔN_{max}

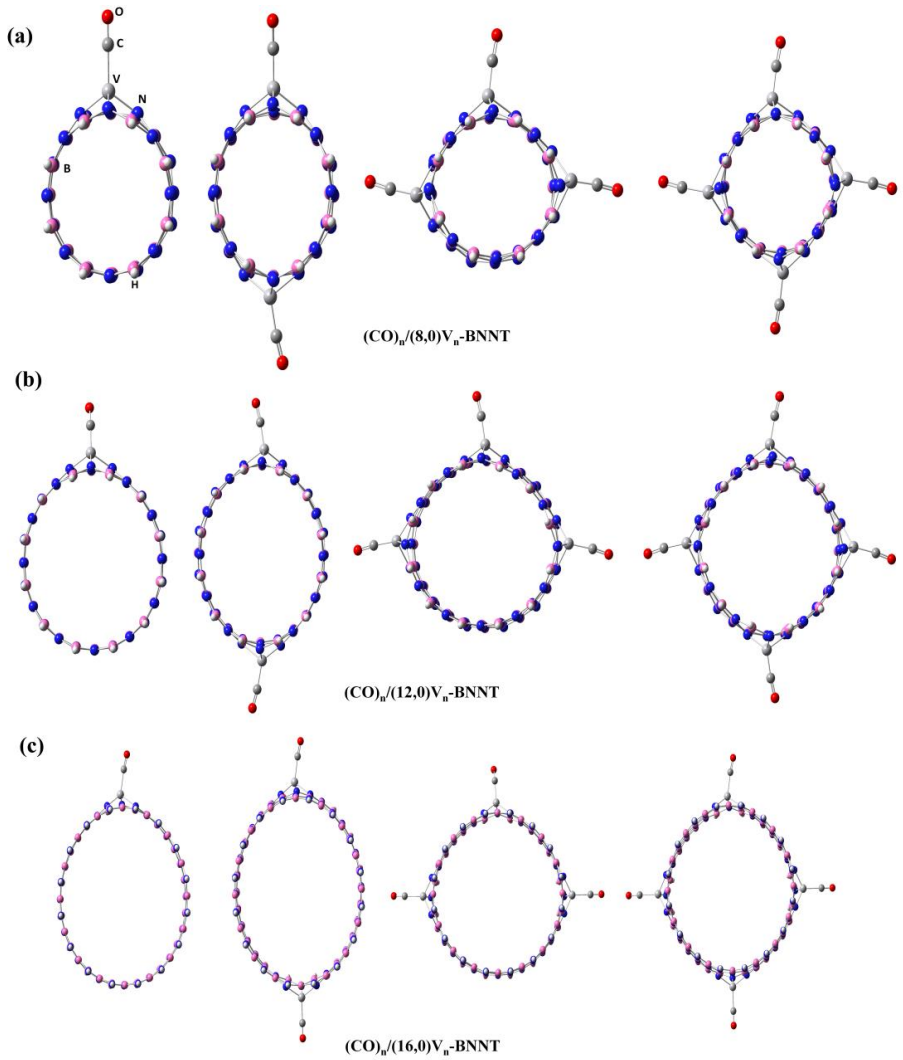

Fig. 3. Optimized structures for a configuration of (a) $(CO)_n/V_n$-(8,0)BNNT, (b) $(CO)_n$/V-(12,0)BNNT, and (c) $(CO)_n$/V-(16,0)BNNT, (n=1-4).

Table 2. The interaction energy (kJ/mol), the C(O)…B distances (d), and the value of charge transfer (CT) from CO to nanotube in $(CO)_n/V_n$-BNNT complexes at the B3LYP/6-311++G(d) level of theory.

Complex	ΔE^{BSSE}	d/(Å)	CT		ΔE^{BSSE}	d/(Å)	CT		ΔE^{BSSE}	d/(Å)	CT
BNNT		(8,0)				(12,0)				(16,0)	
$(CO)_1$/V-BNNT											
a	-144.552	1.960	-0.017	a	-146.271	1.946	-0.201	a	-157.533	1.945	-0.057
b	-51.994	1.995	-0.077	b	-57.593	1.983	-0.100	b	-59.855	1.979	-0.111
$(CO)_2/V_2$-BNNT											
a	-296.680	1.949	-0.778	a	-312.990	1.946	-0.106	a	-314.833	1.945	-0.099
b	-103.991	1.979	-0.231	b	-113.062	1.974	-0.198	b	-117.467	1.971	-0.218
$(CO)_3/V_3$-BNNT											
a	-404.546	1.947	-0.144	a	-470.424	1.946	-0.157	a	-478.262	1.943	-0.189
b	-166.489	1.983	-1.109	b	-172.543	1.980	-0.316	b	-207.528	1.979	-0.443
$(CO)_4/V_4$-BNNT											
a	-622.941	1.948	-0.199	a	-628.204	1.945	-0.214	a	-631.484	1.944	-0.307
b	-228.190	1.977	-0.539	b	-230.085	1.973	-0.432	b	-235.513	1.970	-0.457

Table 3. The molecular descriptors for nanotubes and $(CO)_n$/BNNT complexes in the gas phase at the B3LYP/6-311++G(d) level of theory.

Complex	configuration	Eg(eV)	η(eV)	S(eV)	μ(eV)	ω(eV)	ΔN_{max}(eV)
(8,0) BNNT		5.607	2.803	0.178	-3.615	2.331	1.290
$(CO)_1$/BNNT	a	5.311	2.656	0.188	-3.753	2.652	1.413
	b	5.429	2.714	0.184	-3.706	2.529	1.365
$(CO)_2$/BNNT	a	5.311	2.655	0.188	-3.748	2.645	1.411
	b	5.338	2.669	0.187	-3.721	2.594	1.394
$(CO)_3$/BNNT	a	5.303	2.651	0.189	-3.747	2.648	1.413
	b	5.324	2.662	0.188	-3.715	2.592	1.395
$(CO)_4$/BNNT	a	5.303	2.652	0.189	-3.744	2.644	1.412
	b	5.303	2.651	0.189	-3.709	2.595	1.399
(12,0) BNNT		6.266	3.133	0.160	-3.325	1.765	1.061
$(CO)_1$/BNNT	a	5.370	2.685	0.186	-3.770	2.646	1.404
	b	5.382	2.691	0.186	-3.753	2.617	1.394
$(CO)_2$/BNNT	a	5.374	2.687	0.186	-3.766	2.639	1.401
	b	5.377	2.688	0.186	-3.744	2.606	1.392
$(CO)_3$/BNNT	a	5.373	2.686	0.186	-3.764	2.637	1.401
	b	5.383	2.691	0.186	-3.766	2.635	1.399
$(CO)_4$/BNNT	a	5.373	2.687	0.186	-3.762	2.634	1.400
	b	5.364	2.682	0.186	-3.726	2.588	1.389
(16,0) BNNT		6.192	3.096	0.162	-3.322	1.782	1.073
$(CO)_1$/BNNT	a	5.336	2.668	0.187	-3.747	2.631	1.404
	b	5.347	2.674	0.187	-3.732	2.605	1.396
$(CO)_2$/BNNT	a	5.334	2.667	0.187	-3.745	2.629	1.404
	b	5.363	2.681	0.186	-3.738	2.606	1.394
$(CO)_3$/BNNT	a	5.331	2.666	0.188	-3.743	2.627	1.404
	b	5.334	2.667	0.187	-3.717	2.590	1.394
$(CO)_4$/BNNT	a	5.329	2.665	0.188	-3.741	2.626	1.404
	b	5.345	2.673	0.187	-3.715	2.582	1.390

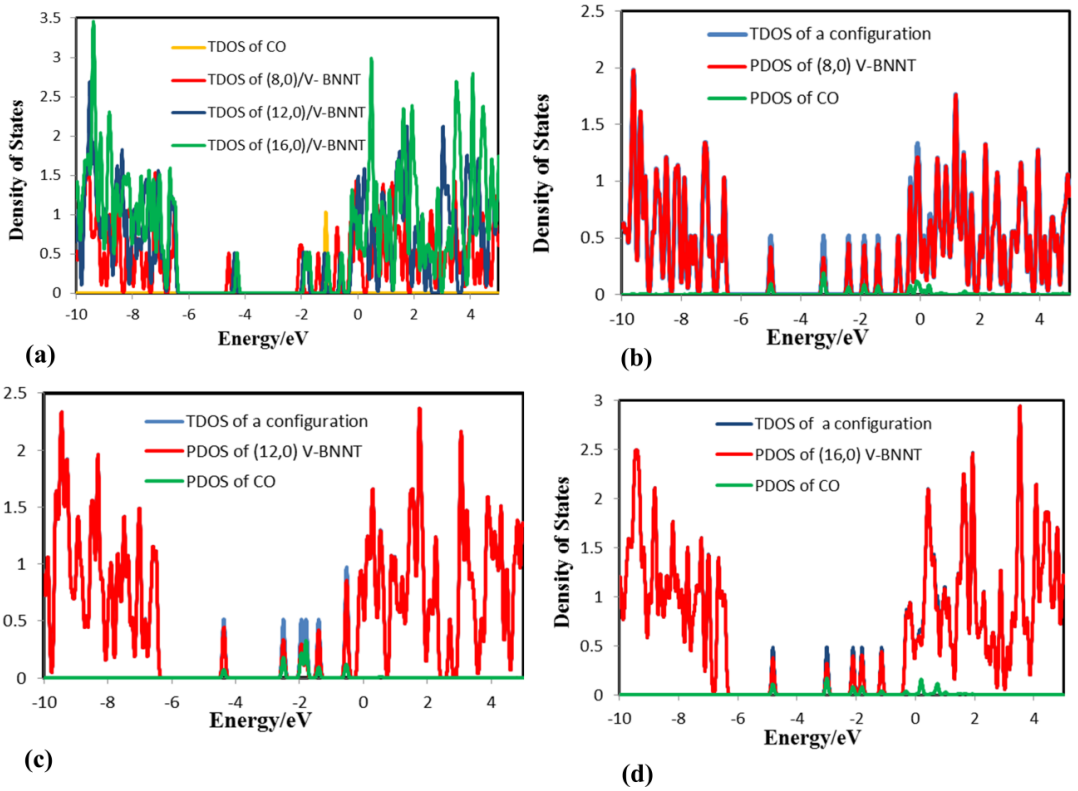

Fig. 4. The total and projected density of states for (a) monomers, (b) $(CO)_1/V_1$-(8,0)BNNT, (c) $(CO)_1/V_1$-(12, 0) BNNT and, (d) $(CO)_1$ / V_1-(16,0)BNNT complexes in a configuration.

Table 4. The molecular descriptors for nanotubes and $(CO)_n/V_n$-BNNT complexes in the gas phase at the B3LYP/6-311++G(d) level of theory.

Complex	Configuration	Eg(eV)	η(eV)	S(eV)	μ(eV)	ω(eV)	ΔN_{max}(eV)
(8,0)V-BNNT		2.504	1.252	0.399	-3.308	4.371	2.642
$(CO)_1$/V-BNNT	a	1.761	0.881	0.568	-4.103	9.556	4.659
	b	1.875	0.938	0.533	-3.570	6.795	3.807
V_2-BNNT		2.486	1.243	0.402	-3.330	4.459	2.678
$(CO)_2/V_2$-BNNT	a	1.640	0.820	0.610	-4.065	10.073	4.956
	b	1.691	0.846	0.591	-3.496	7.228	4.135
V_3-BNNT		2.227	1.113	0.449	-3.335	4.997	2.996
$(CO)_3$/V3-BNNT	a	1.584	0.792	0.631	-4.049	10.349	5.112
	b	1.627	0.813	0.615	-3.795	8.856	4.667
V_4-BNNT		2.176	1.088	0.460	-3.352	5.165	3.081
$(CO)_4/V_4$-BNNT	a	1.581	0.791	0.632	-3.900	9.619	4.933
	b	1.621	0.811	0.617	-3.306	6.740	4.078
(12,0)V-BNNT		2.443	1.222	0.409	-3.132	4.015	2.564
(CO)/V-BNNT	a	1.847	0.924	0.541	-3.871	8.111	4.191
	b	1.857	0.929	0.538	-3.423	6.310	3.686
V_2-BNNT							
		2.375	1.187	0.421	-3.184	4.268	2.681
$(CO)_2/V_2$-BNNT	a	1.834	0.917	0.545	-3.953	8.522	4.311
	b	1.854	0.927	0.539	-3.402	6.244	3.670
V_3-BNNT		2.367	1.183	0.422	-3.146	4.181	2.658
$(CO)_3/V_3$-BNNT	a	1.587	0.794	0.630	-4.007	10.117	5.049
	b	1.811	0.906	0.552	-3.345	6.176	3.693
V_4-BNNT		2.346	1.173	0.426	-3.156	4.245	2.690
$(CO)_4/V_4$-BNNT	a	1.456	0.728	0.687	-3.978	10.868	5.464
	b	1.820	0.910	0.549	-3.314	6.036	3.642
(16,0)V-BNNT		2.425	1.213	0.412	-3.051	3.838	2.516
$(CO)_1$/V-BNNT	a	1.818	0.909	0.550	-3.886	8.307	4.275
	b	1.853	0.927	0.540	-3.351	6.058	3.616
V_2-BNNT		2.427	1.213	0.412	-3.064	3.869	2.525
$(CO)_2/V_2$-BNNT	a	1.814	0.907	0.551	-3.900	8.384	4.300
	b	1.852	0.926	0.540	-3.342	6.030	3.609
V_3-BNNT		2.321	1.161	0.431	-3.028	3.949	2.609
$(CO)_3/V_3$-BNNT	a	1.705	0.853	0.586	-3.921	9.016	4.598
	b	1.833	0.916	0.546	-3.290	5.905	3.590
V_4-BNNT		2.315	1.157	0.432	-3.045	4.004	2.630
$(CO)_4/V_4$-BNNT	a	1.343	0.672	0.744	-3.756	10.505	5.593
	b	1.386	0.693	0.722	-3.543	9.062	5.115

of $(CO)_n/V_n$−BNNT complexes were increased. With the change of the tube diameter, it is not observed the regular change in the electronic properties of $(CO)_n/V_n$−BNNT complexes. Based on Table 3, the energy gap and the chemical hardness of **a** configurations is less than **b** configurations. Therefore, conductivity, chemical softness, the chemical potential, electrophilicity index, and ΔN_{max} of **a** configurations is greater than **b** ones. In comparison with the previous work, the results show that the adsorption of CO molecules on the V_n-BNNTs is stronger than Al-doped and Ga-doped BNNTs [36]. It is predicted that V_n-BNNTs could be a more appropriate option for adsorption of CO molecules. The density of states (DOS) plots for monomers and the most stable configuration of CO/V-BNNT complexes are shown in Fig. 4. Based on the DOS spectra of complexes, the HOMO and LUMO states have been shifted upon complexation. Therefore, in comparison with the V-doped nanotubes, HOMO, and LUMO states of CO/V-BNNT complexes move to more negative energy. These results show that the adsorption of CO molecules on the V-BNNTs leads to a change in the conductivity of the nanotubes.

The charge analysis discloses important details on the electron density transfer (CT) in donor-acceptor interactions (Tables 1 and 2). In the interaction of CO molecules with BN and V_n-BNNTs, the charge transfer occurs between nanotubes and CO molecules. In this work, the charge transfer can be defined as the sum of

Table 5. The molecular descriptor for nanotubes and $(CO)_n/V_n$-BNNT complexes. in the solution phase.

Complex	Configuration	Eg(eV)	η(eV)	S(eV)	μ(eV)	ω(eV)	ΔN_{max}(eV)
(8,0)BNNT	V-BNNT	2.45	1.23	0.41	-2.90	3.43	2.37
$(CO)_1$/V-BNNT	a	1.84	0.92	0.54	-4.01	8.73	4.36
	b	1.95	0.98	0.51	-3.33	5.69	3.42
	V_2-BNNT	2.43	1.22	0.41	-2.91	3.48	2.39
$(CO)_2/V_2$-BNNT	a	1.81	0.90	0.55	-4.01	8.90	4.44
	b	1.72	0.86	0.58	-3.32	6.41	3.85
	V_3-BNNT	2.18	1.09	0.46	-2.84	3.70	2.61
$(CO)_3/V_3$-BNNT	a	1.76	0.88	0.57	-3.92	8.74	4.45
	b	1.81	0.91	0.55	-3.81	8.39	4.40
	V_4-BNNT	2.14	1.07	0.47	-2.84	3.79	2.66
$(CO)_4/V_4$-BNNT	a	1.88	0.94	0.53	-3.89	8.06	4.14
	b	1.64	0.82	0.61	-3.15	6.05	3.85
(12,0) BNNT	V-BNNT	2.39	1.19	0.42	-2.80	3.29	2.35
$(CO)_1$/V-BNNT	a	2.35	1.17	0.43	-4.23	7.62	3.61
	b	1.92	0.96	0.52	-3.25	5.49	3.38
	V_2-BNNT	2.39	1.20	0.42	-2.80	3.28	2.34
$(CO)_2/V_2$-BNNT	a	1.85	0.93	0.54	-3.91	8.26	4.22
	b	1.92	0.96	0.52	-3.25	5.50	3.39
	V_3-BNNT	2.32	1.16	0.43	-2.78	3.34	2.40
$(CO)_3/V_3$-BNNT	a	1.78	0.89	0.56	-3.92	8.62	4.40
	b	1.88	0.94	0.53	-3.21	5.48	3.42
	V_4-BNNT	2.30	1.15	0.43	-2.78	3.35	2.41
$(CO)_4/V_4$-BNNT	a	1.71	0.86	0.58	-3.89	8.83	4.54
	b	1.89	0.94	0.53	-3.20	5.43	3.39
(16,0) BNNT	V-BNNT	2.37	1.18	0.42	-2.78	3.27	2.35
$(CO)_1$/V-BNNT	a	1.84	0.92	0.54	-3.89	8.22	4.23
	b	2.36	1.18	0.42	-2.79	3.28	2.36
	V_2-BNNT	2.36	1.18	0.42	-2.79	3.28	2.36
$(CO)_2/V_2$-BNNT	a	1.84	0.92	0.54	-3.89	8.22	4.22
	b	1.91	0.96	0.52	-3.21	5.40	3.36
	V_3-BNNT	2.35	1.17	0.43	-2.79	3.31	2.38
$(CO)_3$/V3-BNNT	a	1.83	0.91	0.55	-3.93	8.45	4.30
	b	1.16	0.58	0.86	-3.58	11.02	6.16
	V_4-BNNT	2.34	1.17	0.43	-2.78	3.31	2.38
$(CO)_4/V_4$-BNNT	a	1.84	0.92	0.54	-3.89	8.25	4.24
	b	1.89	0.95	0.53	-3.19	5.38	3.37

electronic charges of atoms in CO molecules. In CO/BNNT complexes, charge transfer happened from CO molecules to the nanotubes, while the opposite happened in $(CO)_n/V_n$−BNNT complexes. In CO/BNNT complexes, the value of charge transfer in **b** configurations is smaller than **a** ones. The opposite of this result happened in $(CO)_n/V_n$−BNNT complexes. As shown, by increasing the number of CO molecules, the value of the charge transfer between CO molecules and nanotubes was increased upon complexation.

Solvent effects

Investigations show that the dielectric constant of the solvents can be effected on the relative energies, physicochemical propertyies, and the frontier molecular orbital levels of complexes through the interaction between solvent and solute [50, 51]. To understand the influence of the polar solvent on the physicochemical properties of complexes, quantum molecular descriptors were investigated in the solution phase by the PCM model. Single point calculations in water solvent at B3LYP/6-311++G(d) level of theory were performed on the $(CO)_n/V_n$-BNNT complexes optimized in the gas phase. The results are summarized in Table 5. According to the results, in V_n−BN nanotubes, the energy gap, and the chemical hardness decrease, whereas softness, chemical potential, electrophilicity index, and ΔN_{max} increased in the solution phase relative to the gas phase. These results were reversed in $(CO)_n/V_n$−BNNT complexes. It seems that V_n−BNNTs are softer in the solution than the gas phase.

CONCLUSION

In this research, the effect of the interaction of CO molecules on the molecular descriptors of pure and V_n−doped (8, 0), (12, 0) and (16, 0) BNNTs were investigated. Based on the results, $(CO)_n/V_n$−BNNT complexes are more stable than $(CO)_n$/BNNT ones. By doping of V atoms, the electronic properties of nanotube were changed and the energy gap of complexes decreased. Thus, the conductivity of nanotubes was increased upon complexation. It seems that the V_n−BNNTs could be appropriate for the adsorption of the CO molecules. It obvious that the conductivity and the chemical reactivity of Vn-BNNTs in the soluble phase are greater than the gas phase. According to the NBO results, in CO/BNNT complexes, charge transfer was carried out from CO molecules to nanotubes, while the opposite was observed in $(CO)_n/V_n$−BNNT complexes. The value of charge transfer in $(CO)_n/V_n$−BNNT complexes is more than $(CO)_n$/BNNT. By increasing the number of the CO molecules, the value of charge transfer between CO molecules and nanotubes was increased upon complexation. It is predicted that the V_n-nanotubes with a larger diameter can be a better candidate for the adsorption of the CO molecules. It was found that compared to carbon nanotubes, boron nitride nanotubes are a better candidate for adsorption of the CO molecules [32] and the best pure BN nanotubes for adsorption of the CO molecules, are smaller diameter nanotubes [35, 49]. Also, the interaction of the CO molecule with the V-BNNTs is stronger than Al, Ga, Si-doped BNNTs and weaker than Ni, Pd and Pt-doped boron nitride nanotubes [33-36].

ACKNOWLEDGMENTS

The authors sincerely thank the Sirjan University of Technology and the Payame Noor University and for providing financial support of this work.

CONFLICT OF INTEREST

The authors declare that they have no competing interests.

REFERENCES

[1] Iijima S., (1991), Synthesis of Carbon Nanotubes. *Nature*. 354: 56–58.

[2] Robertson J., (2007), Growth of nanotubes for electronics. *Mater. Today*. 10: 36–43.

[3] Javey A., (2008), The 2008 Kavli Prize in Nanoscience: Carbon Nanotubes. *ACS Nano*. 2: 1329–1335.

[4] Chen Y., Yin S., Li Y., Cen W., Li J., Yin H., (2017), Curvature dependence of single-walled carbon nanotubes for SO2 adsorption and oxidation. *Appl. Surf. Sci*. 404: 364–369.

[5] Hsieh S. C., Wang S. M., Li F. Y., (2011), A theoretical investigation of the effect of adsorbed NO_2 molecules on electronic transport in semiconducting single-walled carbon nanotubes. *Carbon*. 49: 955–965.

[6] Talla J. A., (2012), Ab initio simulations of doped single-walled carbon nanotube sensors. *Chem. Phys*. 392: 71-77.

[7] Xu H., Li l., Fan G., Chu X., (2018), DFT study of nanotubes as the drug delivery vehicles of Efavirenz. *Comput. Theor. Chem*. 1131: 57–68.

[8] Harris P. J. F., (1999). Carbon Nanotubes and Related Structures, Cambridge University Press: Cambridge.

[9] Soltani A., Ramezani Taghartapeh M., Tazikeh Lemeski E. b., Abroudi M., Mighani H., (2013), A theoretical study of the adsorption behavior of N2O on single-walled AlN and AlP nanotubes. *Superlattices Microst*. 58: 178–190.

[10] Soltani A., Ramezani Taghartapeh M., Mighani H., Pahlevani A. A., Mashkoor R., (2012), A first-principles study of the SCN− chemisorption on the surface of AlN, AlP, and BP nanotubes. *Appl. Surf. Sci*. 259: 637– 642.

[11] Zhi C., Bando Y., Tang C., Golberg D., (2010), Boron nitride nanotubes. *Mater. Sci. Eng. Rep*. 70: 92–111.

[12] Bahrami Panah M., Vaziri R., (2015), Structure and electronic properties of single–walled zigzag BN and $B_3C_2N_3$ nanotubes using first-principles methods. *Int. J. Nano Dimens*. 6: 157-165.

[13] Weng Q., Wang X., Wang X., Bando Y., Golberg D., (2016), Functionalized hexagonal boron nitride nanomaterials: Merging properties and applications. *Chem. Soc. Rev*. 45: 3989-4012.

[14] Ciofani G., Raffa V., Menciassi A., Cuschieri A., (2008), Cytocompatibility, interactions, and uptake of polyethyleneimine-coated boron nitride nanotubes by living cells: confirmation of their potential for biomedical applications. *Biotechnol. Bioeng*. 101: 850-858.

[15] Panchal M. B., Upadhyay S., (2014), Boron nitride nanotube-based biosensor for acetone detection: Molecular structural mechanics-based simulation. *Mol. Simulat*. 40: 1035-1042.

[16] Kalay S., Yilmaz Z., Sen O., Emanet M., Kazanc E., Çulha M., (2015), Synthesis of boron nitride nanotubes and their applications. *Beilstein J. Nanotechnol*. 6: 84-102.

[17] Mortazavifar A., Raissi H., Akbari A., (2019), DFT and MD investigations on the functionalized boron nitride nanotube as an effective drug delivery carrier for Carmustine anticancer drug. *J. Mol. Liq*. 276: 577–587.

[18] Meyer N., Bekaert K., Pirson D., Devillers M., Hermans S., (2012), Boron nitride as an alternative support of Pd catalysts for the selective oxidation of lactose. *Catal. Commun*. 29: 170-174.

[19] Khaleghian M., Azarakhshi F., (2019), Theoretical comparison of thermodynamic parameters, NMR analysis, electronic properties of Boron Nitride and Aluminum Nitride nanotubes. *Int. J. Nano Dimens*. 10: 105-113.

[20] Ghosh D., Ghosh B., Hussain S., Chaudhuri S., Bhar R., Pal A. K., (2012), Novel BN/Pd composite films for stable liquid petroleum gas sensor. *Appl.Surf. Sci.* 263: 788-794.

[21] Zhai T., Li L., Ma Y., Liao M., Wang X., Fang X., Yao J., Bando Y., Golbeng D., (2011), One-Dimensional inorganic nanostructures: Synthesis field-emission and

photodetection. *Chem. Soc. Rev*. 40: 2986-3004.
[22] Vessally E., Dehbandi B., Edjlali L., (2016), DFT study on the structural and electronic properties of Pt-doped boron nitride nanotubes. *Russ. J. Phys. Chem. A.* 90: 1217-1223.
[23] Esrafili M. D., Saeidi N., (2017), $N_2O + SO_2$ reaction over Si- and C-doped boron nitride nanotubes: A comparative DFT study. *Appl. Surf. Sci*. 403: 43-50.
[24] Esrafili M. D., Nematollahi P., (2017), Potential of Si-doped boron nitride nanotubes as a highly active and metal-free electrocatalyst for oxygen reduction reaction: A DFT study. *Syn. Met*. 226: 129-138.
[25] Javan M. B., Soltani A., Ghasemi A. S., Lemeski E. T., Gholami N., Balakheyli H., (2017), Ga-doped and antisite double defects enhance the sensitivity of boron nitride nanotubes towards Somanand Chlorosoman. *Appl. Surf. Sci*. 411: 1-10.
[26] Makiabadi B., Zakarianezhad M., Ekrami-Kakhki M. S., Zareye S., (2019), Adsorption of the nitrosamine and thionitrosamine molecules as carcinogen compounds on the BN and B_3Al N nanotubes: ADFT study. *Phosphorus. Sulfur Relat. Elem*. 194: 57-63.
[27] Fan G. H., Zhu S., Li X. K., Ni K., Xu H., (2017), Ab initio investigation of pristine and doped single-walled boron nitride nanotubes as acetone sensor. *Comput. Theor. Chem*. 1115: 208–216.
[28] Abdoli M., Saeidian H., Kakanejadifard A., (2017), The interaction of propargylamine based sulfonamide with pristine, Al and Si-doped boron nitride nanotubes: A theoretical study. *Comput. Theor. Chem*. 1115: 323–329.
[29] Hamadanian M., Fotooh F. K., (2014), Density functional study of Al/N co-doped (10, 0) zigzag single-walled carbon nanotubes as CO sensor. *Comp. Mater. Sci*. 82: 497–502.
[30] Esrafili M. D., Saeidi N., (2017), Healing of a carbon-vacancy defect in silicon carbide nanotubes by CO molecules: A DFT study. *Chem. Phys. Lett*. 671: 49-55.
[31] Singh N. B., Bhattachary B., Mondal R., Sarkar U., (2016), Nickel cluster functionalised carbon nanotube for CO molecule detection: A theoretical study. *Mol. Phys*. 114: 671-680.
[32] Baei M., (2013), Theoretical Study of $(CO)_{n=1,2}$ Adsorption on the (6, 0) Zigzag Single-walled Carbon Nanotube. *Fuller Nanotube Carbon N*. 21: 117–124.
[33] Esrafili M. D., Saeidi N., (2016), DFT calculations on the catalytic oxidation of CO over Si-doped (6, 0) boron nitride nanotubes. *Struct. Chem*. 27: 595-604.
[34] Basharnavaz H., Habibi-Yangjeh A., (2017), A DFT study for adsorption of CO on Ni, Pd, and Pt atoms doped (7, 0) boron nitride nanotube. *Mol. Phys*. 116: 204-211.
[35] Sun M., Xu J., Cui Yu., Wu G., Zhang H., Li Z., (2013), Theoretical study of adsorption CO molecule on Palladium-doped Boron Nitride nanotubes. *Adv. Mater. Res*. 662: 233-238.
[36] Ahmadi-Peyghan A., Soltani A., Pahlevani A. A., Kanani Y., Khajeh S., (2013), A first-principles study of the adsorption behavior of CO on Al- and Ga-doped single-walled BN nanotubes. *Appl. Surf. Sci*. 270: 25–32.
[37] Xie Y., Huo Y. P., Zhang J. M., (2012), First-principles study of CO and NO adsorption on transition metals doped (8, 0) boron nitride nanotube. *Appl. Surf. Sci*. 258: 6391-6397.
[38] Rezazadeh M., Ghiasi R., Jamehbozorgi S., (2018), Solvent effects on the structure and spectroscopic properties of the second-generation anticancer drug carboplatin: A theoretical insight. *J. Struct. Chem*. 85: 245-251.
[39] Fereidoni S., Ghiasi R., Pasdar H., (2018), Theoretical study of the solvent effect on the electronic and vibrational properties of [CpFe(CO)2(NCS)] and [CpFe(CO)2(SCN)] linkage isomers. *J. Struct Chem*. 59: 1058-1066.
[40] Rahimi M., Ghiasi R., (2018), Solvent effect on isomerization reaction of [(η5-C5H5)(CO)2ReC(C2HB10H10)(C6H5)] carbene complex to [(η5-C5H5)(CO)(COC2HB10H10) ReCC6H5] carbyne
complex: A computational investigation. *J. Mol. Liq*. 265: 164-171.
[41] Becke A. D., (1993), Density-functional thermochemistry. III. The role of exact exchange. *J. Chem. Phys*. 98: 5648–5652.
[42] Feller D., (1996), The role of databases in support of computational chemistry calculations. *J. Comp. Chem*. 17: 1571–1586.
[43] Frisch M., Trucks G., Schlegel H. B., Scuseria G., Robb M., Cheeseman J., Scalmani G., Barone V., Mennucci B., Petersson G., (2009), Gaussian 09, Revision A. 02, Gaussian. Inc, Wallingford, CT.
[44] Boys S. F., Bernardi F., (1970), The calculation of small molecular interactions by the differences of separate total energies. Some procedures with reduced errors. *Mol. Phys*. 19: 553-566.
[45] Thiemens M. H., Trogler W. C., (1991), Nylon production: An unknown source of atmospheric nitrous oxide. *Science.* 251: 932-934.
[46] Miertus S., Scrocco E., Tomasi J., (1981), Electrostatic interaction of a solute with a continuum. A direct utilizaion of ab initio molecular potentials for the prevision of solvent effects. *Chem. Phys*. 55: 117-129.
[47] Reed A. E., Curtiss L. A., (1988), Weinhold F., Intermolecular interactions from a natural bond orbital, donor-acceptor viewpoint. *Chem. Rev.* 88: 899-926.
[48] Boyle N., Tenderholt A., Langner K., (2008), Cclib: A library for package-independent computational chemistry algorithms. *J. Comput. Chem*. 29: 839-845.
[49] El-Barbary A. A., Eid Kh. M., Kamel M. A., Taha H. O., Ismail G. H., (2015), Adsorption of CO, CO_2, NO, and NO_2 on Boron Nitride Nanotubes: DFT Study. *J. Surf. Eng. Mater. Adv. Technol*. 5: 154-161.
[50] Rezazadeh M., Ghiasi R., Jamehbozorgi S., (2018), Influence of solvent and electric field on the structure and IR, ^{31}P NMR spectroscopic properties of a titanocene-benzyne complex. *J. Appl. Specrosct*. 85: 526-534.
[51] Mahmoudzadeh G., Ghiasi R., Pasdar H., (2019), Solvent influence on structure and electronic properties of Si2Me4: A computational investigation using PCM-SCRF method. *Russ. J. Phys. Chem. A.* 93: 2244-2249.